Cell

Dysregulation of Cardiogenesis, Cardiac Conduction, and Cell Cycle in Mice Lacking miRNA-1-2

Yong Zhao,[1,2,3,8] Joshua F. Ransom,[1,2,3,8] Ankang Li,[6,7] Vasanth Vedantham,[1,4] Morgan von Drehle,[1] Alecia N. Muth,[1] Takatoshi Tsuchihashi,[1,2,3] Michael T. McManus,[5] Robert J. Schwartz,[6] and Deepak Srivastava[1,2,3,*]

[1] Gladstone Institute of Cardiovascular Disease, 1650 Owens Street, San Francisco, CA 94158, USA
[2] Department of Pediatrics (Cardiology)
[3] Department of Biochemistry and Biophysics
[4] Department of Internal Medicine (Cardiology)
[5] Diabetes Center
University of California, San Francisco, San Francisco, CA 94143, USA
[6] Institute of Biosciences and Technology, Texas A & M Health Science Center
[7] Graduate Program in Cardiovascular Sciences, Baylor College of Medicine, Houston, TX 77030, USA
[8] These authors contributed equally to this work.
*Correspondence: dsrivastava@gladstone.ucsf.edu
DOI 10.1016/j.cell.2007.03.030

SUMMARY

MicroRNAs (miRNAs) are genomically encoded small RNAs used by organisms to regulate the expression of proteins generated from messenger RNA transcripts. The in vivo requirement of specific miRNAs in mammals through targeted deletion remains unknown, and reliable prediction of mRNA targets is still problematic. Here, we show that miRNA biogenesis in the mouse heart is essential for cardiogenesis. Furthermore, targeted deletion of the muscle-specific miRNA, miR-1-2, revealed numerous functions in the heart, including regulation of cardiac morphogenesis, electrical conduction, and cell-cycle control. Analyses of miR-1 complementary sequences in mRNAs upregulated upon *miR-1-2* deletion revealed an enrichment of miR-1 "seed matches" and a strong tendency for potential miR-1 binding sites to be located in physically accessible regions. These findings indicate that subtle alteration of miRNA dosage can have profound consequences in mammals and demonstrate the utility of mammalian loss-of-function models in revealing physiologic miRNA targets.

INTRODUCTION

Many complex cellular, developmental, and homeostatic processes depend on precise spatiotemporal regulation of protein levels, some of which function as "rheostats" to execute programs in a quantitative fashion. The dose-sensitivity of proteins involved in the development and maintenance of organs is highlighted by the numerous human diseases caused by heterozygous mutations that result in haploinsufficiency (http://www.ncbi.nlm.nih.gov/entrez/query.fcgi?db=OMIM). This is particularly true for the heart. The heart is one of the most conserved organs at the molecular level (Buckingham et al., 2005; Olson, 2006; Srivastava, 2006) and is the organ most affected by disease in childhood and adult populations (Thom et al., 2006). Human heart disease can involve abnormalities in morphogenesis, muscle maintenance and function, and cardiac rhythm. Damage to heart muscle is typically irreversible as cardiomyocytes terminally exit the cell cycle postnatally and have little or no regenerative capacity, despite niches of cardiac progenitors that may contribute to basal turnover of myocytes (Torella et al., 2006; Soonpaa and Field, 1998). Networks of transcription factors regulate heart development and maintenance in a dose-dependent manner, but the effects of translational regulation on the titration of these pathways are largely unknown.

MicroRNA (miRNA)-mediated control of protein expression is likely a widely used mechanism for posttranscriptional regulation of important cellular pathways (Ambros, 2004; Kloosterman and Plasterk, 2006; Zhao and Srivastava, 2007). Nearly 500 mammalian miRNAs are transcribed in the nucleus and undergo successive processing events by the enzymes Drosha and Dicer to ultimately yield mature miRNAs of ~20–22 nucleotides (Berezikov et al., 2006). Mature miRNAs typically bind to target mRNAs by partial sequence matching after becoming incorporated into the RNA-induced silencing complex (RISC), resulting in degradation of the mRNA transcript and/or translational inhibition. Disruption of miRNAs in *Caenorhabditis elegans* and *Drosophila* suggest several

ways by which miRNAs may control cellular events. In some cases, they function to "fine-tune" physiologic events, but in others they function as molecular "switches" (Brennecke et al., 2003; Johnston and Hobert, 2003; Kwon et al., 2005; Lee et al., 1993; Moss et al., 1997; Reinhart et al., 2000; Sokol and Ambros, 2005; Wightman et al., 1993). miRNAs can also function in a "fail-safe" mechanism to silence mRNAs that are unwanted in specific cell lineages (Cohen et al., 2006; Hornstein et al., 2005). In mice, interference with miRNA biogenesis by tissue-specific deletion of *Dicer* revealed a requirement of miRNA function during limb outgrowth (Harfe et al., 2005) and in development of skin progenitors (Yi et al., 2006). However, the in vivo requirement of specific miRNAs in mammals through targeted deletion remains unknown.

We and others have described muscle-specific miRNAs, such as the bicistronic miR-1 and miR-133 cluster and miR-206. miR-1 and -133 are expressed in cardiac and skeletal muscle and are transcriptionally regulated by the myogenic differentiation factors MyoD, Mef2, and serum response factor (SRF) (Chen et al., 2006; Kwon et al., 2005; Lagos-Quintana et al., 2001; Rao et al., 2006; Sokol and Ambros, 2005; Zhao et al., 2005). An ancient genomic duplication likely resulted in two distinct loci for the miR-1/miR-133 cluster in vertebrates, with identical mature sequences derived from the duplicated loci. In *Drosophila*, deletion of the single *miR-1* gene (*dmiR-1*), expressed specifically in cardiac and somatic muscle, results in a defect in muscle differentiation or maintenance (Kwon et al., 2005; Sokol and Ambros, 2005). *dmiR-1* targets the Notch ligand, Delta, a known regulator of cardiogenesis and myogenesis in flies (Kwon et al., 2005). In contrast, overexpression of miR-1 in mouse cardiac progenitors has a negative effect on proliferation, where it targets the transcription factor Hand2, which is involved in myocyte expansion (Zhao et al., 2005). Similar to the heart, miR-1 overexpression in cultured skeletal myoblasts promotes skeletal muscle differentiation, as does the related but skeletal muscle-specific miR-206 (Chen et al., 2006; Kim et al., 2006). miR-133 overexpression curiously prevents skeletal muscle differentiation, suggesting that differential processing from the dicistronic transcript may regulate cellular decisions of differentiation or proliferation (Chen et al., 2006). Although significant dysregulation of miRNA expression has been reported in cardiac disease (Sayed et al., 2007; van Rooij et al., 2006), it remains unknown if the heart requires miRNA function for normal development or maintenance.

A major obstacle in understanding how miRNAs regulate cellular events has been identifying mRNAs that are directly targeted by a specific miRNA. While a few targets have been validated at the protein level for miR-1 and several other miRNAs, each miRNA likely targets tens of different mRNAs (Brennecke et al., 2005; Lewis et al., 2005; Rajewsky, 2006). Bioinformatic approaches rewarding a high-degree of Watson-Crick base-pairing at nucleotides 2–7 at the 5′ end of the miRNA (the so-called "seed match") and its mRNA target have been informative, but specificity remains a problem in efficiently identifying targets (Didiano and Hobert, 2006; Lewis et al., 2005; Rajewsky, 2006). We proposed that accessibility of the miRNA binding site within the mRNA, as defined by the local secondary structure and free energy characteristics of the mRNA, may be an important predictor of true miRNA:mRNA interactions (Zhao et al., 2005). We had found that most validated miRNA targets exist in locally accessible regions of mRNAs, although mammalian targets have generally been validated in overexpression models that may not accurately reflect endogenous requirements (Zhao and Srivastava, 2007). The true importance of target accessibility in mammalian physiologic settings has awaited generation of in vivo loss-of-function models to better ascertain criteria for miRNA:mRNA interactions at a genome-wide level.

In this report, we examine the effects of a global loss of miRNAs during cardiac development and use targeted deletion to examine the requirement of a specific miRNA, miR-1-2. We demonstrate that the functions of miR-1 are dose sensitive and that miR-1-2 regulates cardiac morphogenesis, cardiac conduction, and the cardiac cell cycle. Using the loss-of-function model, we characterize miR-1-2 targets and evaluate the importance of miRNA target accessibility along with seed matching in determining miRNA targets.

RESULTS

Disruption of the *Dicer* Allele in Cardiac Progenitors

To assess the global requirement of miRNAs in the mouse heart, we deleted a floxed *Dicer* allele (Harfe et al., 2005), using Cre recombinase under control of the endogenous *Nkx2.5* regulatory region, which directs expression in cardiac progenitors by embryonic day (E) 8.5 (Moses et al., 2001). *Dicer*, which is essential for processing of pre-miRNAs into the mature form (Bernstein et al., 2001), was efficiently deleted in the heart, and the embryos died from cardiac failure by E12.5 (Figure 1). Embryos lacking Dicer in the developing heart exhibited pericardial edema and a poorly developed ventricular myocardium. Most markers of initial cardiac differentiation and patterning, such as Tbx5, Hand1, Hand2, and Mlc2v, were expressed normally (Figure 1). Microarray analysis of E11.5 hearts in triplicate, before obvious signs of dysfunction, revealed upregulation of several genes, such as the endoderm marker α fetoprotein and the skeletal muscle-specific gene, fast skeletal troponin; numerous genes were also downregulated, including those encoding the homeodomain only protein (Hop), myoglobin, and the potassium channel Kcnd2 (Table S3). The early lethality in the *Dicer* mutant revealed an essential requirement for miRNA function in the developing heart.

One of the most abundant and specific miRNAs affected in the *Dicer* mutant heart was miR-1. miR-1-1 and miR-1-2 are both specific for cardiac and skeletal muscle and are cotranscribed as dicistronic messages with miR-133a-2 and miR-133a-1, respectively, but have

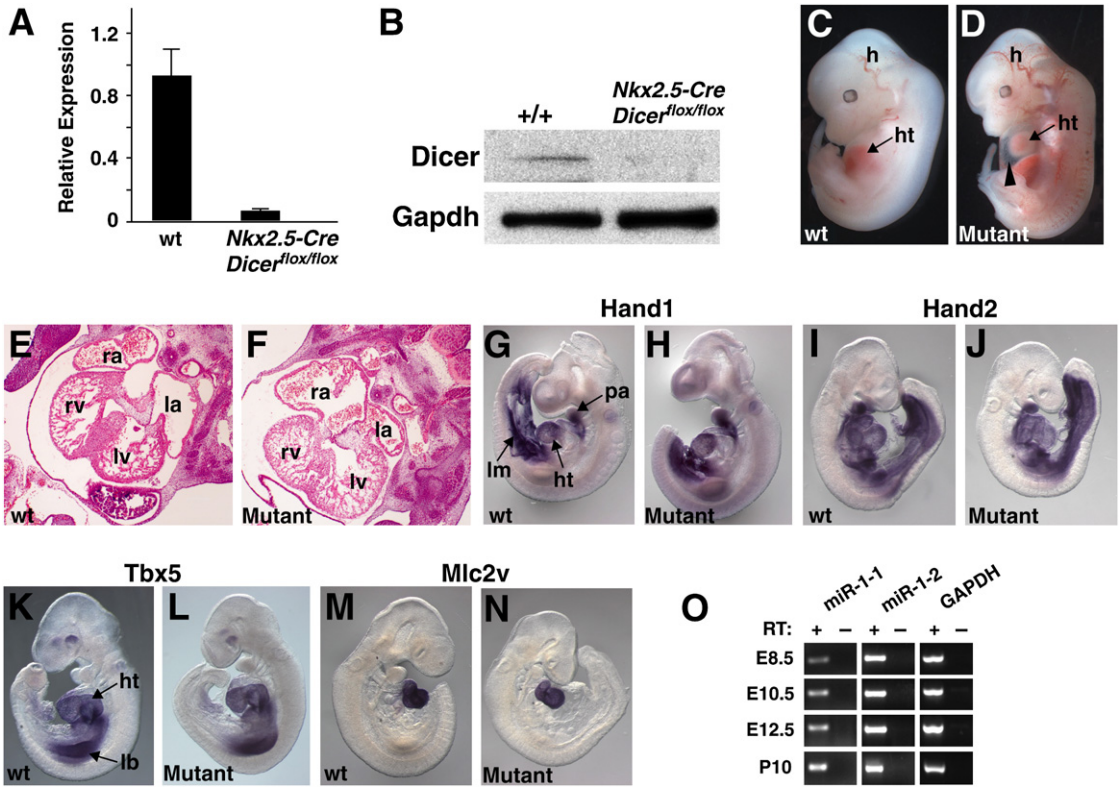

Figure 1. miRNA Biogenesis Is Necessary for Cardiogenesis

(A) Quantitative RT-PCR for relative mRNA levels of Dicer's RNase III domain.

(B) Protein level of Dicer in wild-type (wt) or *Nkx2.5-Cre*; *Dicer*^{flox}/*Dicer*^{flox} embryos measured by western blot using an antibody that recognizes the RNase III domain.

(C and D) *Nkx2.5-Cre*; *Dicer*^{flox}/*Dicer*^{flox} (mutant) embryos showed developmental delay and pericardial edema (arrow) at E12.5.

(E and F) Transverse sections of E11.5 embryos showing thin-walled myocardium in mutant.

(G–N) Whole-mount in situ hybridization with indicated cardiac markers in wild-type and mutant E9.5 embryos.

(O) RT-PCR using primers specific for miR-1-1 or miR-1-2 in wild-type hearts at E8.5, E10.5, E12.5, and P10 with or without reverse transcriptase (RT).

ra, right atrium; la, left atrium; rv, right ventricle; lv, left ventricle; h, head; ht, heart; pa, pharyngeal arch; lm, lateral mesoderm; lb, limb bud.

unique expression patterns (Chen et al., 2006; Wienholds et al., 2005; Zhao et al., 2005). Using PCR primers specific for each miRNA, we found that both were present in the embryonic and postnatal heart, although miR-1-2 expression began slightly earlier in the embryonic heart (Figure 1).

Targeted Deletion of *miR-1-2* in Mice

To define the in vivo function of a specific miRNA in mammals, we targeted the 21-nt mature *miR-1-2* sequence for deletion by homologous recombination in mouse embryonic stem (ES) cells. *miR-1-2* is transcribed as a 2.5 kilobase (kb) message containing miR-1-2 and miR-133a-1 sequences (Chen et al., 2006). The *miR-1-2*/*miR-133a-1* gene resides in a 14.6 kb genomic region between the 12th and 13th exons of the *Mind bomb1* (*Mib1*) locus, involved in Notch signaling (Koo et al., 2005), in an antisense orientation, and is regulated by an independent SRF-dependent enhancer in the heart and MyoD-dependent enhancer in skeletal muscle (Figure 2) (Zhao et al., 2005). Gene targeting was designed to remove the mature 21 nt *miR-1-2* sequence, while leaving the rest of the transcribed sequence, enhancer region, and *Mib1* exons intact (Figure 2).

Mice heterozygous for *miR-1-2* survived without any apparent abnormalities and reproduced efficiently. *miR-1-2* heterozygotes were intercrossed, and in the surviving homozygous mutants, we confirmed the absence of the miR-1-2 transcript with PCR primers specific for the pre-form of miR-1-2. The miR-133a-1 pre-form was transcribed intact, and we did not detect compensatory changes in miR-1-1 levels. Importantly, Mib1 transcript levels were unchanged in the *miR-1-2* mutant with efficient transcription through the targeted locus, as determined by quantitative real-time RT-PCR (qPCR) using primers crossing the exons 19 and 20 (Figure 2). RT-PCR across the exons 12 and 13 revealed normal splicing of exons surrounding the targeted locus (Figure 2). Thus, we specifically targeted the *miR-1-2* locus without affecting nearby genes.

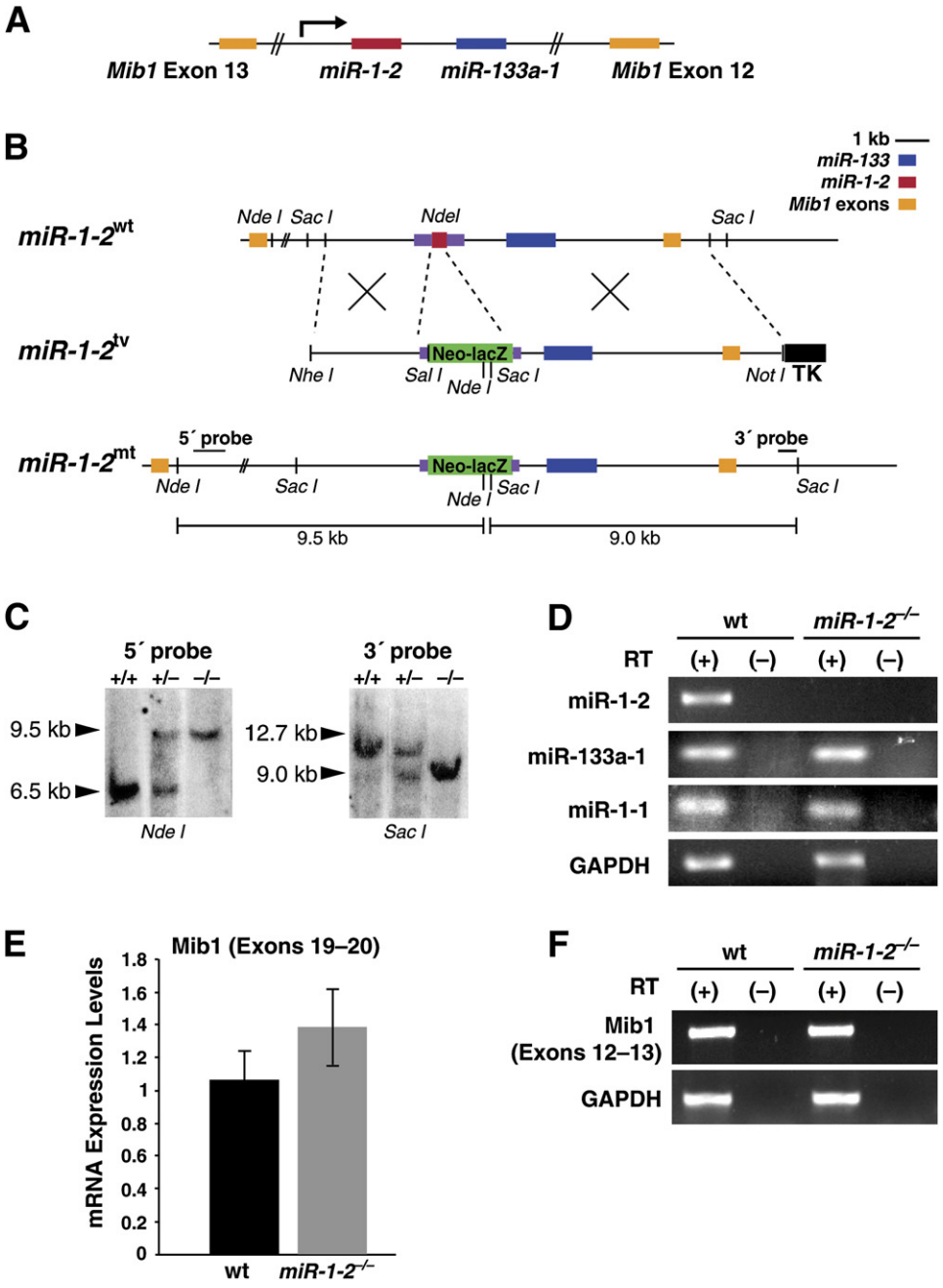

Figure 2. Generation of Mice with Targeted Deletion of *miR-1-2*

(A) Schematic of the *miR-1-2* and *miR133a-1* locus between the 12th and 13th exons of *Mind bomb1* (*Mib1*); arrow indicates direction of transcription of the miRNAs, opposite of *Mib1* transcription.

(B) Targeting strategy for deletion of *miR-1-2* by replacement of 21 nucleotides with the *Neomycin* (*Neo*) resistance cassette using homologous recombination. The wild-type (wt) and mutant (mt) loci are shown with the targeting vector (tv). Mature miR-1-2 sequence is indicated in red, pre-miR-1-2 in purple. TK, thymidine kinase.

(C) Genomic Southern analysis of wild-type (+/+), *miR-1-2* heterozygous (+/–), or homozygous (–/–) mice using 5′ or 3′ probes, after digestion of genomic DNA with *Nde* I or *Sac* I, respectively.

(D) RT-PCR of wild-type and *miR-1-2*-null hearts showing specific loss of *miR-1-2* in comparison to *miR-133a-1* and absence of miR-1-1 upregulation.

(E) Real-time qPCR results in wt or mutant hearts showing intact transcription of the *Mib1* gene using primers 3′ of the miRNA locus (exons 19 and 20). Data are presented as means ± standard error of the mean (SEM).

(F) RT-PCR using primers spanning exons 12 and 13 showing normal splicing across the targeted region.

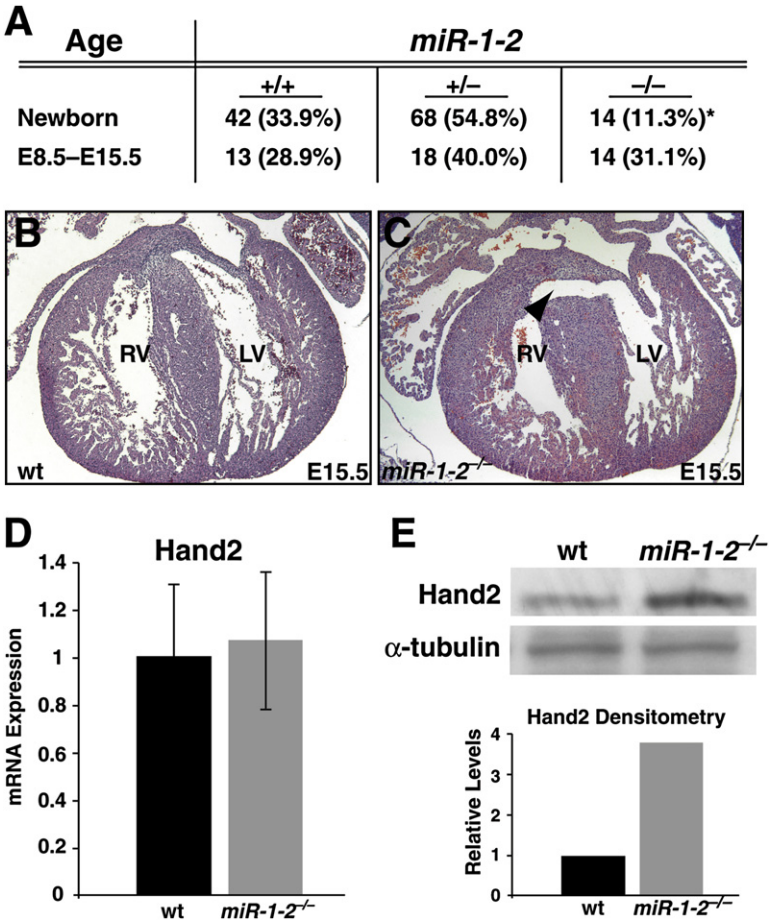

Figure 3. Partial Penetrance of Cardiac Morphogenetic Defects in *miR-1-2* Mutants

(A) Genotypes of mice from *miR-1-2*$^{+/-}$ intercrosses. Absolute numbers are shown with percentages in parenthesis. *$p < 0.025$.

(B and C) Transverse sections of wild-type (wt) or *miR-1-2*$^{-/-}$ hearts at E15.5 showing ventricular septal defect (arrowhead).

(D) qPCR of Hand2 showing similar levels of Hand2 mRNA in *miR-1-2* mutant and wt hearts. Data are presented as means ± SEM.

(E) Western blot of protein lysate from wt or mutant hearts showing increased Hand2 protein level in mutant, quantified by densitometry. rv, right ventricle; lv, left ventricle.

Cardiac Morphogenetic Defects in *miR-1-2* Mutants

Genotyping of offspring from *miR-1-2* heterozygous intercrosses revealed 50% lethality by weaning (Figure 3). Mendelian ratios were observed in offspring until E15.5, but thereafter, death occurred at varying times, ranging from E15.5 to just after birth. The external anatomy of mutant embryonic hearts was unremarkable, except for occasional enlargement. Skeletal muscle was grossly normal. However, histologic analysis revealed a large ventricular septal defect (VSD) in half of the embryos (Figure 3). Failure of ventricular septation results in death within hours after birth in mice, but some *miR-1-2*$^{-/-}$ embryos also exhibited pericardial edema before birth, consistent with primary myocardial dysfunction in utero contributing to embryonic demise. VSDs can result from dysregulation of myriad events during cardiogenesis, and it is likely that miR-1-2 regulates numerous genes during this process. Our previous studies demonstrated a highly conserved miR-1 binding site in the 3′UTR of a critical cardiac transcription factor, Hand2, that responded to overexpression of miR-1 by inhibiting translation (Zhao et al., 2005). Precise dosage of Hand2 is essential for normal cardiomyocyte development and morphogenesis (McFadden et al., 2005; Srivastava et al., 1995, 1997; Yamagishi et al., 2001; Yelon et al., 2000). The mRNA levels of Hand2 were unchanged in *miR-1-2* mutants, but the protein levels were increased approximately 4-fold as seen by western blots (Figure 3), consistent with Hand2 being a physiologic miR-1 target in vivo.

Cardiac Electrophysiologic Defects in *miR-1-2* Mutants and miR-1-2 Regulation of Irx5

The *miR-1-2* homozygous mice that survived postnatally exhibited a range of phenotypes. In some cases (~15%), mice developed rapid dilation of the heart and ventricular dysfunction with evidence of atrial thrombi and death by 2–3 months of age. The rest were remarkably normal with no dysfunction by echocardiography nor evidence of scarring, but many suffered sudden death. Because abnormalities in cardiac conduction and repolarization often cause sudden death, we performed surface electrocardiography in mutant mice and their littermates. The average heart rate of mutants was significantly lower than that of wild-type littermates, and the normal delay between atrial and ventricular depolarization (the PR interval) was shortened (Figure 4). In addition, ventricular depolarization, manifested by the QRS complex, was significantly prolonged in the mutant hearts. Synchronous depolarization of ventricular myocytes is coordinated by rapid conduction

A

Parameter	*miR-1-2* +/+ (n = 7)	+/– (n = 9)	–/– (n = 12)	*P* value
Heart Rate (bpm)	459 ± 12	483 ± 11	411 ± 15*	0.03
PR Interval (msec)	35.5 ± 0.6	35.4 ± 0.6	33.4 ± 0.5*	0.03
QRS Interval (msec)	10.7 ± 0.3	10.8 ± 0.2	12.3 ± 0.3*	0.004
QT Interval (msec)	57 ± 2	55 ± 1	64 ± 1*	0.01
QTc	50 ± 2	50 ± 1	52 ± 1	0.3

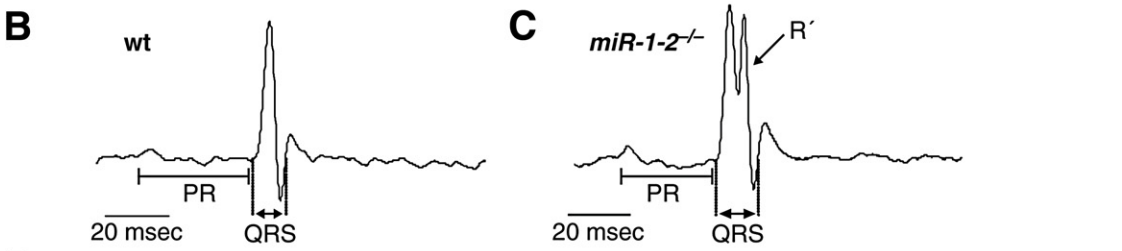

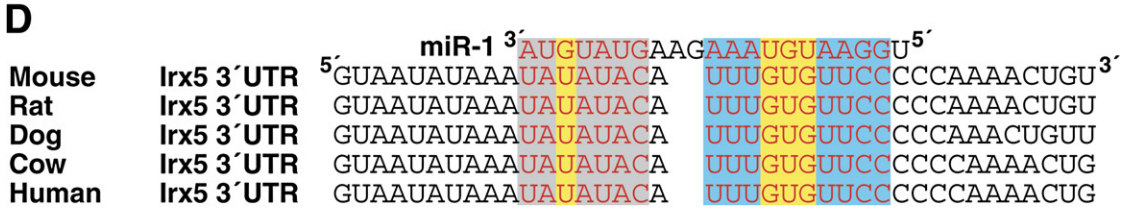

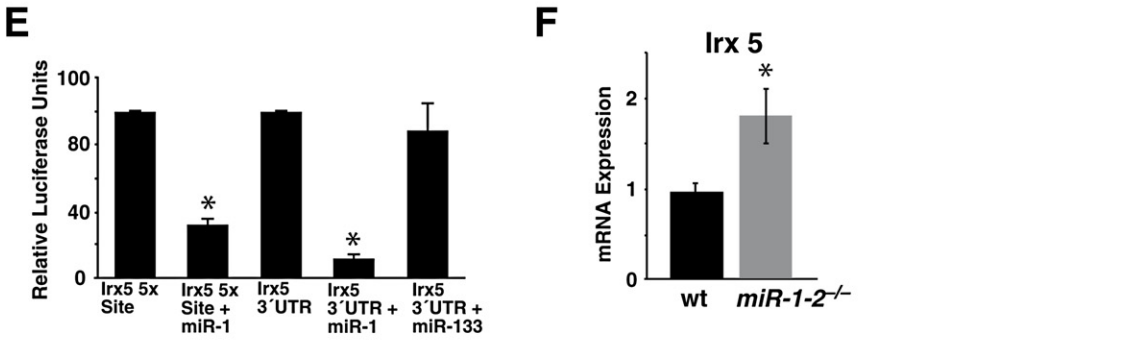

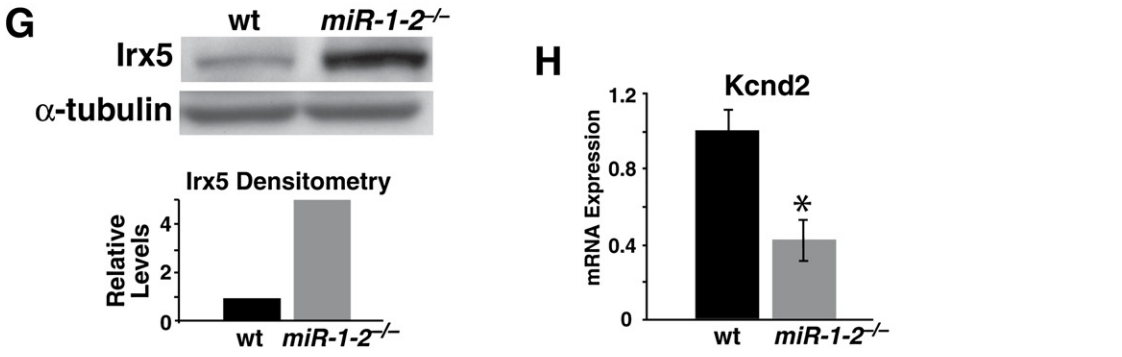

Figure 4. Cardiac Electrophysiologic Defects in *miR-1-2* Mutants and miR-1-2 Regulation of Irx5

(A) Electrocardiographic parameters of wild-type (+/+), *miR-1-2*$^{+/-}$, and *miR-1-2*$^{-/-}$ adult mice. $P < 0.05$ was considered significant. bpm, beats per minute; msec, milliseconds.

(B and C) Representative diagrams of electrocardiograms in lead II indicate the location of PR and QRS intervals. The second peak in the QRS complex (R′) was observed in 58% of mutant and only 14% of wild-type mice ($p < 0.05$).

(D) Sequence alignment between miR-1 and the 3′UTR of Irx5 in several species. 5′ seed matching is shown with Watson-Crick base-pairing in blue and non-Watson-Crick G::U wobble in yellow; sequence matching in the 3′ end is boxed in light gray.

through the atrioventricular bundle, bundle branches, and Purkinje fibers. The increased width and the morphology of the QRS complex in the mutants were typical of abnormal conduction along one of the bundle branches (bundle-branch block), a finding that in humans can be associated with an increased risk of sudden death (Desai et al., 2006).

In our search for potential miR-1 targets that might explain aspects of the cardiac conduction abnormalities, we found that the 3′UTR of Irx5 had a well-conserved miR-1 binding site (Figure 4) and was located in a region of very high free energy (ΔG) (5′ ΔG: −8.5 and 3′ ΔG: −2.8), suggesting a locally accessible site. Irx5 belongs to the Iroquois family of homeodomain-containing transcription factors and regulates cardiac repolarization by repressing a key potassium channel, Kcnd2 (Costantini et al., 2005). We therefore cloned the miR-1 binding site (five copies) from the Irx5 3′UTR or the entire Irx5 3′UTR into the luciferase reporter 3′UTR, with transcription of luciferase under control of a constitutively active thymidine kinase promoter. Introduction of these reporter plasmids into tissue-culture cells resulted in high levels of luciferase activity. Addition of miR-1 into this system resulted in a significant reduction in luciferase activity, which was specific for miR-1, as introduction of miR-133 did not result in a significant change in activity (Figure 4). Since miRNAs can repress protein production by affecting either mRNA stability or translation, we assessed both mRNA and protein levels in *miR-1-2* mutant hearts. qPCR revealed a nearly 2-fold increase in Irx5 mRNA levels in *miR-1-2*-null hearts compared to wild-type, and western blots showed an approximately 5-fold increase in Irx5 protein accumulation by densitometry (Figure 4). Consistent with the upregulation of Irx5, we found that transcripts of the Irx5 target gene *Kcnd2* were downregulated in the mutant hearts (Figure 4). These data provide compelling evidence that miR-1 regulates the cardiac electrical system and directly targets Irx5.

miR-1-2 Regulates Cardiac Cell Cycle and Karyokinesis

Although the vast majority of adult *miR-1-2* mutants had normal cardiac function, we often observed thickening of the walls of the heart by echocardiography. We confirmed this observation by assessing the heart-to-body weight ratios of mice sacrificed at 4–6 months of age. The mutant mice had a significant increase in this ratio (Figure 5). Histologic analysis revealed no evidence of myocyte hypertrophy or fibrosis, suggesting that the increased weight may be due to hyperplasia. Dissociation of heart muscle in wild-type and mutants and assessment of cell number revealed a 20% increase in the number of cardiomyocytes in *miR-1-2*-null mice (Figure 5). The normal variance among animals was minimal, and this represented a significant degree of hyperplasia ($p < 0.001$). Closer histologic examination of the adult hearts revealed that many myocytes appeared to be undergoing nuclear division. Immunohistochemistry with antibodies recognizing phosphohistone H3 (PH3) (Wei et al., 1998), a marker for mitotic nuclei, and cardiac α-actinin to mark cardiomyocytes, revealed the unusual presence of mitotic adult cardiomyocytes (Figure 5). Postnatal mouse cardiomyocytes typically undergo a single round of nuclear and sometimes cellular division in the first two weeks of life, before terminally exiting the cell cycle (Li et al., 1996). At postnatal day 10 (P10), we consistently found a significant increase in PH3-positive myocytes (~3-fold, $p < 0.02$), indicating increased proliferation in the *miR-1-2* mutants (Figure 5). PH3-positive myocytes—never observed in adult wild-type mice—were found in 2–3-month-old mutant animals, although the number of PH3-positive cells was highly variable, ranging from a few cells to the large number of cells indicated in a highly affected adult *miR-1-2* mutant heart.

Enrichment of miR-1 Seed Matches among mRNAs Upregulated in *miR-1-2* Mutants

A major benefit of studying mice that lack a specific miRNA is the ability to investigate mRNAs that may be upregulated upon loss of function of the miRNA, a subset of which may be direct miRNA targets. These would represent targets regulated at the level of mRNA stability rather than via translational inhibition (Valencia-Sanchez et al., 2006). To address this, we performed mRNA expression microarray analyses of P10 wild-type and mutant hearts, well before any obvious dysfunction. Forty-five protein-coding genes were significantly upregulated and 25 downregulated in *miR-1-2*-null hearts (Figure 6). The dysregulated genes clustered into several major categories, including upregulation of cardiac transcription factors, such as Irx5 (as described above), Irx4, Hrt2, Hand1, and Gata6. In addition, we observed upregulation of numerous cell-cycle regulators and concomitant downregulation of tumor suppressor genes (Figure 6). qPCR of candidate dysregulated genes validated over 80% of those tested, suggesting that the subtle dysregulation of numerous regulatory genes may contribute to the *miR-1-2* mutant cardiac irregularities. qPCR data of a subset of cell cycle and tumor-suppressor genes and genes encoding cardiac transcription factors are consistent with the proliferative phenotype of the mutant (Figure 6).

If some of the mRNAs upregulated upon *miR-1-2* deletion were direct targets, we would expect a disproportionate percentage of sequence complementarity with miR-1

(E) Luciferase activity in Cos cells with the Irx5 miR-1 binding site (5x) or 3′UTR of Irx5 cloned into the luciferase 3′UTR. Values relative to luciferase reporter alone are shown. Data are presented as means ± SEM.

(F) qPCR of Irx5 mRNA in wt or *miR-1-2* mutants showing 1.8-fold increase in mutants (n = 3).

(G) Western blot of protein lysates of postnatal day 10 (P10) wt or *miR-1-2* mutant hearts with Irx5- or α-tubulin-specific antibodies showing an increase in Irx5 protein in mutants, quantified by densitometry.

(H) qPCR of the Irx5 target gene, *Kcnd2*, showing downregulation in the *miR-1-2* mutant. Data are presented as means ± SEM. *$p < 0.05$.

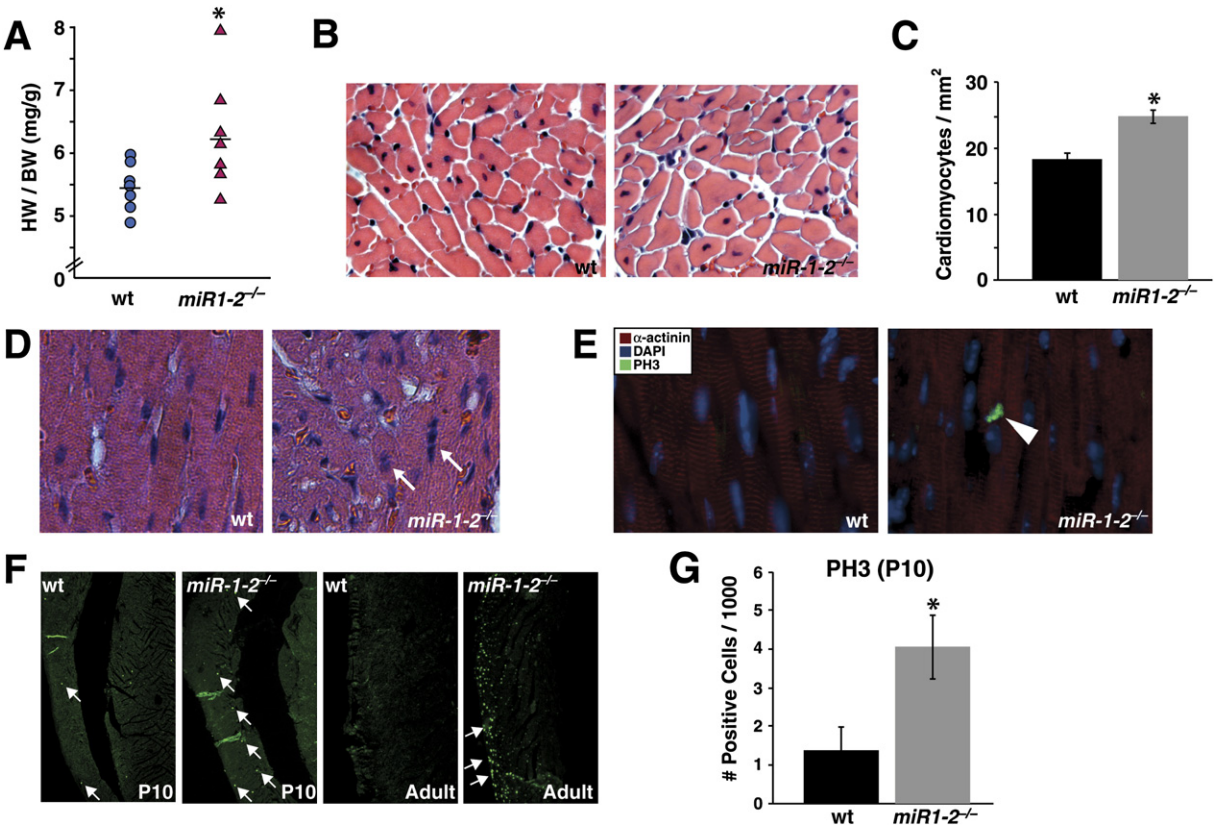

Figure 5. Cardiomyocyte Hyperplasia and Proliferation in *miR-1-2* Mutants

(A) The heart weight-to-body weight (HW/BW) ratio was greater in *miR-1-2*$^{-/-}$ adult mice than in wild-type (wt) mice with data from individual mice shown. Bars indicate averages, *p < 0.05.

(B) Coronal sections stained with H&E showing similar cardiomyocyte diameter between adult wt and *miR1-2*$^{-/-}$ hearts and lack of hypertrophy.

(C) Quantitation of cardiomyocyte number from dissociated wt or *miR-1-2*$^{-/-}$ adult hearts (n = 3).

(D) H&E of cardiac sections from adult hearts suggestive of mitotic nuclei in *miR-1-2*$^{-/-}$ animals (white arrows).

(E) Immunohistochemistry using phosphohistone H3 (PH3, green), α-actinin (red), or DAPI (blue) antibodies demonstrating PH3-positive cardiomyocytes in the adult *miR-1-2* mutant.

(F) Coronal sections of P10 and adult hearts showing an increase in the number of PH3^{+} nuclei in mutants compared to wt.

(G) Quantification of PH3^{+} nuclei per section of P10 heart, showing average of multiple sections each from five wt or *miR-1-2* mutant mice. Data are presented as means ± SEM. *p < 0.05.

in their 3′UTRs (Lim et al., 2005). We therefore analyzed the 3′UTRs for Watson-Crick base-pairing with varying stretches of residues between nucleteotides 1 and 8 of miR-1, encompassing the seed match. We compared the occurrence of motifs that had sequence matching with 5′ or 3′ regions of miR-1 in mRNAs upregulated or downregulated in *miR-1-2* mutants with the frequency of such motifs in over 26,000 mRNA 3′UTRs encoded by the mouse genome. We did the same analysis for enrichment of seed matches with a second miRNA, miR-124, as a control.

There was no statistical enrichment for miRNA complementarity among mRNAs downregulated in mutants. However, we observed significant enrichment for matches with miR-1 positions 1–8, 2–8, 2–7, and 1–7 among mRNAs upregulated in *miR-1-2* mutants (Figure 7) ($p < 0.001$). An upward slope in the graphical depiction (Figures 7B–7D) of tabular data indicates enrichment of miR-1 seed matches in upregulated genes. Although nearly 50% of upregulated genes had 2–7 seed matches, the six-nucleotide complementarity did not effectively discriminate between up- and downregulated genes. However, 12 of 45 upregulated mRNAs (27%) had a miR-1 match of at least seven nucleotides in the 5′ region compared to 2 of 25 in the downregulated group ($p < 0.0001$). No enrichment of 3′-sequence matches was observed in the upregulated genes. As an important control, there was no enrichment for 5′ matches of miR-124 with the upregulated genes in the *miR-1-2* mutant (Figure 7).

Accessibility of miRNA Binding Sites Defined by Local Free Energy

The degree of Watson-Crick base-pairing, particularly at the 5′ end of the miRNA, is a major criterion in defining

A

	Genes Dysregulated in *miR-1-2*$^{-/-}$	
	Upregulated	Downregulated
Cell cycle and/or associated with tumor	Gadd45b Trp53inp2 Runx1 Hlf protamine1 Rbbp9 Mt1 Netrin-1 Map2k5 Igsf4c Efna5 Efnb3	Lck Rad51l1 Arhgap20 Fbxw7 Lrrc3b
Cardiac growth and/or differentiation	Hrt2 Ror1 Gata6 Mov10l1	Nppb
Cardiac conduction system/ ventricular repolarization/ ion channels-associated gene	Irx5 Irx4 Cacna1c	Atp1a2 Kcnd2 Hamp1

B

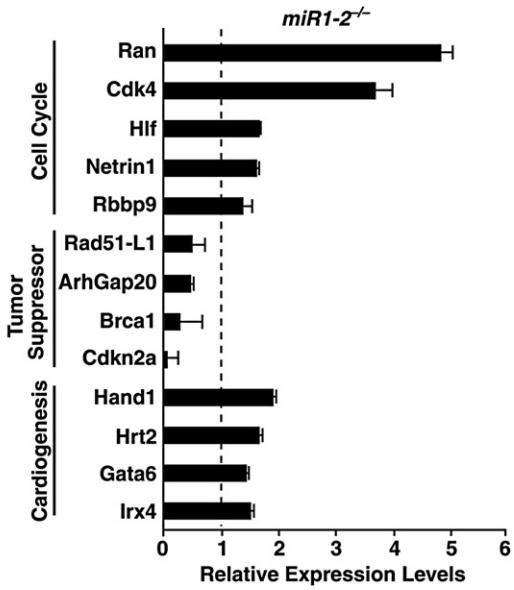

Figure 6. Dysregulated Genes in *miR-1-2*$^{-/-}$ Hearts

(A) Genes that were consistently up- or downregulated in the *miR1-2*$^{-/-}$ hearts at P10 by microarray analysis.

(B) Validation of gene dysregulation in *miR-1-2*$^{-/-}$ P10 hearts compared to wt by qPCR. Data are presented as means ± SEM. Dotted line indicates wt expression levels for each gene set at one.

miRNA:mRNA interactions (Lewis et al., 2005; Rajewsky, 2006; Stark et al., 2003). However, many mRNA targets predicted by sequence matching fail validation tests in vivo (Didiano and Hobert, 2006; Zhao et al., 2005). There is increasing recognition that contextual features may also govern this interaction (Ambros, 2004; Du and Zamore, 2005; Vella et al., 2004). Earlier, we proposed physical accessibility of the mRNA target region as a potential contextual feature and found that nearly all miRNA targets validated at the level of protein regulation were located preferentially in regions of high free energy and unstable secondary structure (Zhao et al., 2005). Quantification of the ΔG for 70 nucleotides flanking each side of the miRNA binding site and evaluation of the secondary structure of the target site itself allowed establishment of potential criteria to enhance target prediction. Since few miRNA targets have been described in mammals, the validity of this model remains uncertain.

The generation of *miR-1-2* mutants provided an opportunity to test whether upregulated mRNAs that contain seed matches are more frequently located in high ΔG areas than would be expected randomly. We calculated the ΔG of 70 nt immediately flanking the 5′ and 3′ sides of each miR-1 binding site in mRNAs upregulated in *miR-1-2* mutants and determined if it was above or below the species average (ΔG = −13.4). The ratio of regions flanking miR-1 binding sites with higher than average free energy compared to those with lower than average free energy was quantified as the "free energy index." In mice, there is a relatively equal distribution of high or low ΔG regions among 70 nucleotide 3′UTR fragments, resulting in an average index of 1.17 among 100 randomly selected sequences. However, among the mRNAs upregulated in the *miR-1-2* mutant, the index was 6.69, indicating significant enrichment of miR-1 binding sites that are located in more accessible regions (Figures 8 and S1 [$p < 0.01$] and Table S1).

We extended the evaluation of this index to other targets that have been validated in (1) miRNA loss-of-function models in vivo or (2) in reporter assays involving endogenous rather than overexpressed miRNAs, given the potential for nonphysiologic interactions upon overexpression (Didiano and Hobert, 2006). The free energy index in validated *C. elegans* miRNA targets was 5.67 (species average, 0.92; $p < 0.001$), suggesting that these targets were also preferentially located in accessible regions as defined by the free energy of flanking regions (Figures 8 and S2). In *Drosophila*, the index was 3.0 for validated targets (species average, 0.67), but the number of targets was insufficient for statistical analysis. Evaluation of a number of other miRNA targets validated at the protein level in tissue culture or through overexpression studies revealed that they, too, were almost always in areas with at least one high ΔG flanking region (Table S2).

The recent in vivo experimental testing of 16 specific *C. elegans* lsy-6 target sites with perfect seed pairing revealed striking discordance between the predicted and validated lsy-6 binding sites, although the reason for this

A

Motif Occurrence in 3′-UTRs

	Mouse mRNAs (n=26,968) (%)	Dysregulated mRNAs in *miR-1-2*$^{-/-}$ Upregulated (n=45) (%)	*P* value	Downregulated (n=25) (%)	*P* value
miR-1					
5′ region					
1–8 nt	2.1	8.8	0.0015	0.0	1.000
2–8 nt	5.9	20.0	0.0011	4.0	0.0714
1–7 nt	6.5	20.0	0.0002	4.0	0.8137
2–7 nt	18.0	48.9	0.0001	32.0	0.0661
3′ region					
14–21 nt	1.2	2.2	0.4192	0.0	1.0000
14–20 nt	4.0	8.9	0.1047	0.0	1.0000
15–21 nt	4.8	4.4	0.6427	12.5	0.1161
15–20 nt	17.1	20.0	0.3604	20.0	0.4294
miR-124					
5′ region					
1–8 nt	1.6	0.0	1.0000	4.0	0.3318
2–8 nt	7.8	8.9	0.4700	16.0	0.1262
1–7 nt	7.0	4.4	0.8325	8.0	0.5304
2–7 nt	77.1	53.3	0.9999	52.0	0.9986

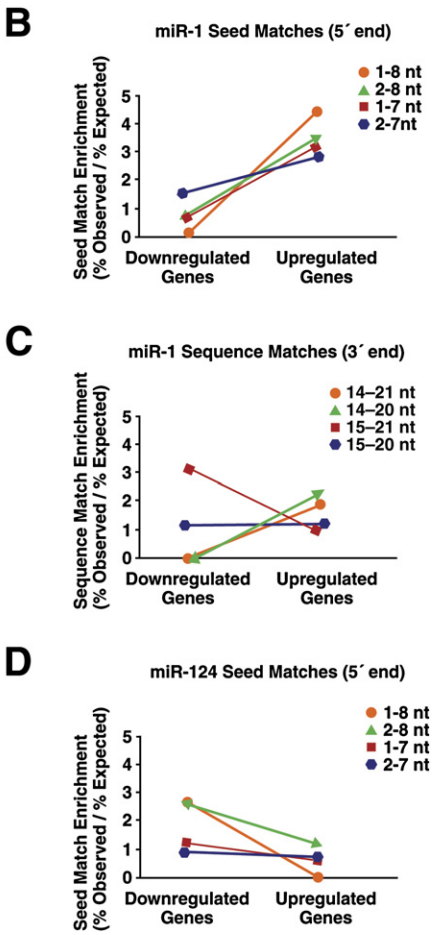

Figure 7. Enrichment of miR-1 5′ Seed Matches among Genes Upregulated in *miR-1-2*$^{-/-}$ Hearts

(A) Table showing the occurrence of miR-1 sequence matches in 3′UTRs of all mRNAs of the mouse genome compared to genes up- or downregulated in *miR-1-2*$^{-/-}$ hearts at P10. The occurrence of motifs that had sequence matching with 5′ or 3′ regions of miR-1 is shown. Similar analysis for miR-124 was performed as a control. P values represent comparison with the genome-wide analysis.

(B–D) Graphical depiction of the enrichment of miR-1 or miR-124 sequence matches among genes up- or downregulated in *miR-1-2* mutants versus the expected number from the mouse genome. A positive slope is indicative of enrichment of sequence matching in the upregulated versus downregulated genes.

discrepancy was unclear (Didiano and Hobert, 2006). We tested the utility of the free energy index on the experimentally validated (2 of 16) or nonvalidated (14 of 16) lsy-6 targets. The index among nonvalidated sites was 1.33 (close to species average), while both validated sites were in very high ΔG regions (Figure 8). This evaluation suggests a strong predictive value of the index, at least in this setting, and may explain why certain lsy-6 predicted targets were not true targets in vivo based on target site accessibility.

DISCUSSION

In this report, we demonstrate that miRNA function in cardiac progenitors is necessary for cardiogenesis and show that disruption of just one of the two *miR-1* family members, *miR-1-2*, has profound consequences for development and maintenance of the heart. Mice lacking *miR-1-2* have a spectrum of abnormalities, including VSDs in a subset that suffer early lethality, cardiac rhythm disturbances in those that survive, and a striking myocyte cell-cycle abnormality that leads to hyperplasia of the heart with nuclear division persisting postnatally. Remarkably, a redundant *miR-1-1* locus did not compensate for loss of *miR-1-2*, at least for many aspects of its function. While it is likely that mice lacking both *miR-1-1* and *miR-1-2* will have even more profound abnormalities, the range of defects upon deletion of *miR-1-2* highlights the ability of miRNAs to regulate multiple diverse targets in vivo. Using the loss-of-function model, we determined in vivo miR-1-2 targets, including the cardiac transcription factor, Irx5, and used this model to evaluate the importance of miRNA target accessibility and of seed matching in determining miRNA targets.

A

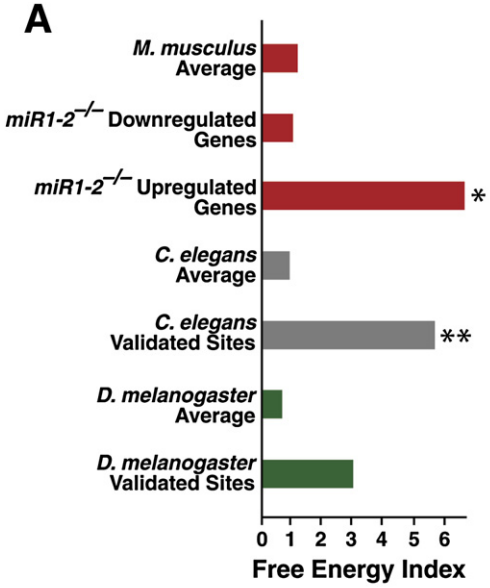

B

Organism	miRNA	Target	Site	5′ 70 bp (ΔG)	3′ 70 bp (ΔG)	Validation method
C. elegans (avg. ΔG=–7.2)	lin-4	*lin-14*	I	–7.7	–3.4	1
			II	–7.8	–1.5	
			III	–2.6	–4.2	
			IV	–5.0	–8.3	
			V	–4.2	–10.6	
			VI	–9.3	–8.7	
			VII	–3.2	–3.0	
		Lin-28	I	–0.6	–10.1	1
	let-7	*lin-41*	I	–0.6	–7.6	1
			II	–9.4	–7.2	
		daf-12	I	–1.6	–10.2	1
			II	–8.9	–1.1	
		pha-4	I	–10.1	–3.9	1
			II	–6.5	–6.6	
		lss-4	I	–17.6	–3.5	1
			II	–9.2	–1.8	
		lin-57	I	–1.5	–3.9	1
			II	–8.1	–8.8	
			III	–5.9	–4.7	
			IV	–2.3	–0.7	
			V	–0.3	–0.1	
			VI	–0.2	–0.3	
			VII	–0.7	–3.8	
			VIII	–0.3	–9.0	
		Ras	I	–1.4	–1.9	1
			II	–2.0	–6.5	
		Nhr-25	I	–6.5	–7.1	1
			II	–4.2	–1.0	
			III	–4.6	–0.5	
		Die-1	I	–15.8	–4.5	1
			II	–2.2	–0.4	
		T14B1.1	I	–7.7	–4.9	2
			II	–4.1	–0.2	
			III	–4.9	–0.3	
		C35E7.4	I	–2.8	–1.8	2
		UNC-129	I	–4.0	–0.7	2
	lsy-6	*cog-1*	I	–1.1	–1.7	1
	miR-273	*Die-1*	I	–3.8	–0.3	2
			II	–4.1	–5.5	
	miR-61	*Vav-1*	I	–0.7	–3.2	2
Drosophila (avg. ΔG=–8.5)	miR-7	*Yan*	I	–5.2	–1.5	1
			II	–4.5	–7.0	
	miR-278	*Expand*	I	–16.3	–6.1	1
			II	–6.6	–5.6	

C

Targets with complementary lsy-6 site	Validation in vivo	5′ 70 bp (ΔG)	3′ 70 bp (ΔG)
cog-1	Yes	–1.1	–1.7
Lin-28 (with lsy-6 binding site)	Yes	–0.3	–0.8
CO2B8.4	No	–6.0	–5.5
F55G1.12	No	–9.1	–5.6
T23E1.1	No	–6.9	–20.5
T14G12.2	No	–6.5	–6.9
Cct-1	No	–8.5	–8.4
T04C9.2	No	–9.9	–10.7
C27H6.3	No	–6.6	–13
C48.D5.2	No	–2.4	–11.7
T20G5.9	No	–11.4	–10.2
R07E3.5	No	–5.4	–7.6
F59A6.1	No	–6.9	–6.8
F40H3.4	No	–6.1	–6.3
ZK637.13	No	–6.5	–6.6
Unc54 (with lsy-6 binding site)	No	–1.5	–11.2

Figure 8. Bias of miRNA Target Sites to "Accessible" Regions Defined by High Free Energy

(A) Free energy index of miR-1 binding sites was defined by flanking regions (70 nucleotides) adjacent to either side of the binding site with calculated free energy (ΔG) above the species average (mouse ΔG = −13.4) divided by the number of flanking regions below the average. *$p < 0.01$, **$p < 0.001$.

(B) List of miRNAs and their target sites within direct mRNA targets validated in vivo. The ΔG of 70 nt genes flanking each miRNA binding site on the 5′ or 3′ side is shown. Validation method by protein levels in loss-of-function models (1) or by repression of reporters by endogenous levels of miRNA activity (2) is indicated.

(C) Analysis of free energy surrounding experimentally validated and nonvalidated *lsy-6* targets in vivo (Didiano and Hobert, 2006). The two validated targets were in much higher ΔG regions than either the *C. elegans* average (−7.2) or the nonvalidated targets, all of which were in low ΔG regions.

miR-1-2 Regulates Cardiac Morphogenesis

In animals and in humans, increases in copy number or gain-of-function mutations can be as consequential as loss of function, sometimes causing similar phenotypes (Liao et al., 2004; Redon et al., 2006). The sensitivity of the heart to gene or protein dosage is reflected in the nearly 1% of live human births that are affected by cardiac malformations, with ventricular septal defects being the most frequent (Hoffman et al., 2004). Interestingly, many genes that cause VSDs when deleted in mice were upregulated in the *miR-1-2* mutants. These included Hrt2/Hey2, a member of the Hairy family of transcriptional repressors that mediates Notch signaling (Fischer and Gessler, 2003; Nakagawa et al., 1999), which itself causes heart disease (Garg et al., 2005), and Hand1, a bHLH transcription factor involved in ventricular development and septation (McFadden et al., 2005; Srivastava et al., 1995). Hand2, a close relative of Hand1, was not upregulated at the mRNA level, but the Hand2 protein levels were increased, consistent with our previous report that miR-1

directly targets Hand2 for translational repression (Zhao et al., 2005). *Hand2* and *Hand1* are partially redundant and progressive loss of the four combined alleles causes increasingly severe heart defects, suggesting that proper titration of Hand dosage is important for cardiogenesis (McFadden et al., 2005). Gata6, a transcription factor partially redundant with Gata4 (Xin et al., 2006), was also upregulated. GATA4 heterozygosity in humans causes VSDs, suggesting this family of genes also plays a role in ventricular septation (Garg et al., 2003). Subtle dysregulation of numerous developmental genes may contribute to the embryonic defects observed in *miR-1-2* mutants.

miR-1-2 Regulation of Cardiac Conduction

Disruptions in cardiac rhythm are frequent causes of sudden death in humans and frequently require placement of pacemakers and defibrillators (Zipes and Wellens, 1998). In *miR-1-2* mutants, we observed an abnormality in the propagation of cardiac electrical activity despite normal anatomy and function. Normally, depolarization and repolarization of cardiomyocytes are determined by the properties of a specialized network of cardiomyocytes, the cardiac conduction system (Gourdie et al., 1999). The transcriptional regulation of these cells requires precise dosages of several transcription factors (Cheng et al., 2003). One of these factors, Irx5, functions with the corepressor Smyd1 to repress the potassium channel, Kcnd2, in an endocardial-to-epicardial transmural gradient within ventricular myocytes (Costantini et al., 2005; Gottlieb et al., 2002). Loss of Irx5 disrupts this pattern, resulting in ventricular repolarization abnormalities and a predisposition to arrhythmias.

Of particular relevance to the findings in the *mir-1-2* mutants, combined loss of function of Irx5 and Irx4 causes prolongation of the PR interval (B.G. Bruneau, personal communication). We showed that *miR-1-2* mutants have the opposite phenotype, with a shortened PR interval, and that Irx5 is a direct target of miR-1. The increase in protein levels of Irx5 in *miR-1-2* mutants was greater than the increase in mRNA levels, raising the possibility that miR-1-2 may regulate both mRNA translation and stability via the Irx5 3′UTR, although this may simply reflect an accumulation of protein. The increase in Irx5 protein levels in *miR-1-2* mutants corresponded to a decrease in the Irx5 target gene, *Kcnd2*, as expected, as well as increased Irx4 mRNA levels. The decrease in Kcnd2 was also observed in *Dicer* mutant embryos, likely due to loss of miR-1.

In addition to the short PR interval, electrocardiography also revealed a broad QRS complex with features of bundle branch block, which can be associated with sudden death in humans, although the contribution of Irx5 dysregulation to this feature remains to be tested.

Cell-Cycle Dysregulation in *miR-1-2* Mutants

miR-1-2 mutants displayed an increase in mitotic nuclei at P10 that continued to varying degrees, even in the adult. The hyperplasia of mutant hearts and the upregulation of genes that promote the cell cycle were consistent with *miR-1-2*-mediated regulation of cell-cycle events in the mammalian heart. Manipulation of the cardiac cell cycle could potentially stimulate the regenerative capacity of the heart, but this has proved challenging given the stringent cell-cycle control in cardiomyocytes (MacLellan and Schneider, 2000). Karyokinesis in differentiated cardiomyocytes is not normally observed. In *miR-1-2* mutants, karyokinesis occurs in the adult heart, and the general molecular "threshold" for cell cycling may be lower, given the upregulation of cell-cycle genes and downregulation of tumor suppressors. While we observed an increased number of cardiomyocytes in the hearts of adult mutants, this is likely a result of the early increase in proliferation, as we do not have evidence that cytokinesis persists in the adult. Consistent with our findings, overexpression of miR-1 and the related miR-206 in skeletal myoblasts results in inhibition of DNA synthesis and withdrawal from the cell cycle (Kim et al., 2006). It will be interesting to determine if the cell cycle threshold is also affected in *miR-1-2* mutant cardiac progenitor cells as they begin to differentiate into myocytes, possibly allowing greater expansion of such cells after injury.

Sequence Matching and Target Site Accessibility during miRNA:mRNA Interactions

Some features of miRNA:mRNA interactions have been revealed through elegant bioinformatics and experimental approaches (Lewis et al., 2005; Stark et al., 2003; Xie et al., 2005), but the limited number of validated miRNA targets reflects our incomplete knowledge of the "rules" of miRNA target prediction. Base-pairing between nucleotides 2–7 of the miRNA and its target site is important. However, many conclusions regarding base-pairing have been drawn from overexpression of miRNAs, in which nonphysiologic miRNA:mRNA interactions may occur and siRNA-like off-target effects may be observed (Birmingham et al., 2006; Jackson et al., 2006).

The *miR-1-2*$^{-/-}$ mouse model described here provided a unique model to address the question of endogenous targets in a mammalian model. Our findings that mRNAs upregulated in hearts lacking *miR-1-2* were enriched for sequence matches with miR-1 nt 1–8, 1–7, or 2–8 was consistent with the concept of seed-match significance. As suggested by previous studies, matches to only 2–7 occurred with higher frequency than would be expected in upregulated genes, but this feature was not useful in discriminating between up- and downregulated genes in the *miR-1-2*$^{-/-}$ model, suggesting that a 7 nt match may be more predictive .

Another potential feature of miRNA:target site interactions may involve local accessibility of the binding site. Significant portions of mRNA sequences are hidden, and only local single-strand regions are accessible for binding to single-strand RNA. Thus, complex RNA secondary structures may have inhibitory effects on miRNA:mRNA interactions. In earlier work, we found that validated miRNA target sites typically had destabilizing elements

or had high free energy in regions flanking the 5′ or 3′ ends of the target site (Zhao et al., 2005). Several additional miRNA targets have been validated in vivo, and we continue to find that most miRNA binding sites reside in areas of high free energy. Analysis of upregulated mRNAs in *miR-1-2* mutants that contain miR-1 binding sites revealed a strong bias toward sites in areas of high free energy. We attempted to quantify this bias with a free energy index that allows determination of the likelihood that target sets are located in accessible areas and therefore may be more likely to be true targets. Analysis of putative *C. elegans* lsy-6 targets provided further evidence of flanking free energy as a criterion for target prediction (Didiano and Hobert, 2006). Indeed, insertion of a lsy-6 binding site into a favourable free energy region of lin-28 allowed targeting by lsy-6, but introduction of an equally matched lsy-6 site into a lower free energy area of unc-54 did not result in effective targeting. Our findings suggest that RNA accessibility, as assessed by free energy of flanking regions, may be a critical feature of miRNA target recognition. The accessibility of an mRNA binding site may be a factor that is regulated by cells via RNA binding proteins or other mechanisms that modulate RNA secondary structure. This may be analogous to DNA binding proteins that function as transcriptional regulators only when local chromatin modifications render *cis* elements accessible for interaction with transcription factors. RNA accessibility as a criterion for target recognition, if upheld as more targets are identified and validated, has the potential to rapidly accelerate the pace of biological discovery related to miRNA biology, as specificity of target prediction has been one of the most significant obstacles in this nascent field.

EXPERIMENTAL PROCEDURES

Generation of *Dicer* Conditional Null or *miR-1-2*-Null Mice

Dicer$^{flox/flox}$ mice (Harfe et al., 2005) and *Nkx2.5-Cre* mice (Moses et al., 2001) have been described previously and were intercrossed to generate *Nkx2.5-Cre*; *Dicer*$^{flox/flox}$ mice. Genotyping was performed as described. To generate *miR-1-2*-null mice, Sv129 embryonic stem (ES) cells were electroporated with the targeting vector. *Nde* I or *Sac* I digests of genomic DNA were used for Southern blot genotyping of 5′ or 3′ recombination, respectively. Two of the 1500 colonies screened were properly targeted and injected into C57BL6 blastocysts to generate high-percentage chimeras that were bred to recover heterozygous mice with germline transmission.

RNA In Situ Hybridization, Quantitative Real-Time PCR, and RT-PCR Analysis

RNA in situ hybridizations of whole embryos were performed as described (Yamagishi et al., 2003). qPCR was performed using the ABI 7900HT (TaqMan, Applied Biosystems) per the manufacturer's protocols. Primer sets for *Mib1* spanned exons 19 and 20 (Taqman: Mm00523008_m1) or exons 12 and 13; sequences are found in Supplemental Data. Expression levels were normalized to Gapdh expression. Semiquantitative RT-PCR was done in the linear range of amplification. Statistical analysis was performed using the two-tailed student's t test.

Immunohistochemistry and Western Blot Analysis

Histological sectioning and hematoxylin and eosin staining were performed according to standard practices. Immunohistochemistry was performed on paraffin embedded sections (7 μm) as described in Supplemental Data. Western blots were performed as described previously (Zhao et al., 2005) on heart tissues from P10 mice. Irx5 antibody (kindly provided by C.C. Hui) was used at 1:100 dilution, goat polyclonal Hand2 (Santa Cruz Biotechnology) at 1:100 dilution, and Dicer C-20 antibody (Santa Cruz Biotechnology) at 1:100 dilution.

Quantification of Cardiomyocyte Cell Numbers

Cardiomyocytes from adult hearts were isolated as previously described using an alkaline dissociation method (Shin et al., 2002). Cell suspension (10 μl) was loaded onto a Fuchs-Rosenthal counting chamber (Hausser Scientific). Cardiomyocytes in the counting chamber were distinguished from fibroblasts by cytoplasmic size and the presence of sarcomeres. The numbers of cardiomyocytes per mm^2 of the counting chamber were evaluated eight times per heart (n = 3).

Sequence Analysis and Free Energy Calculations

Mouse 3′UTR sequences were retrieved from the RefSeq database (http://www.ncbi.nlm.nih.gov/RefSeq/). Bioinformatic analyses of miRNA binding sites were performed as described with ΔGs determined using mFold (Zhao et al., 2005). Determination of motif occurrence is described in Supplemental Data.

Noninvasive Assessment of Heart Function

Transthoracic echocardiography was used for noninvasive serial assessment of cardiac function in mice using a Vevo 770 ultrasound machine (VisualSonics). Cardiac electrophysiological function was assessed by surface electrocardiograms as described in Supplemental Data. Mean, standard deviation, and standard error of the mean were calculated for each genotype, and all pairwise statistical comparisons were made with t tests.

Cell Culture and Transfection Assays

Irx5 3′UTR was cloned into a pGL-TK vector as described (Zhao et al., 2005) and introduced into Cos cells with or without a plasmid containing miR-1 or miR-133. Luciferase assays were performed as described previously (Zhao et al., 2005).

Microarray Analysis

Mouse genome-wide gene expression analysis was performed using Affymetrix mouse genome 430 2.0 array. RNA was extracted from E11.5 or P10 whole heart tissue using Trizol reagent (Invitrogen) per manufacturer's protocol. Microarray analysis was performed in triplicate from independent biologic samples according to the standard Affymetrix GeneChip protocol. Data were analyzed with GeneSpring software (Agilent Technologies). Details of statistical analyses can be found in Supplemental Data.

Supplemental Data

Supplemental Data include two figures, three tables, Supplemental Experimental Procedures, and Supplemental References and can be found with this article online at http://www.cell.com/cgi/content/full/129/2/303/DC1/.

ACKNOWLEDGMENTS

The authors thank K. Ivey and B.G. Bruneau for helpful discussions and critical review of the manuscript, B. Harfe (University of Florida, Gainesville, Florida) for generously providing *Dicer* mutant mice, W. Yu for technical assistance, G. Howard for editorial assistance, P. Ursell (UCSF) for assistance with pathological analyses, S. Morton and J. Morton for help with statistical analyses, B. Taylor for preparation of graphics and manuscript, and C.C. Hui (Hospital for Sick Children, Toronto) for the Irx5-specific antibody. Y.Z. is a postdoctoral scholar of the California Institute of Regenerative Medicine. V. V. was supported by NIH (T32HL007731) D.S. is supported by grants from the NHLBI/NIH, March of Dimes Birth Defects Foundation and is an

Established Investigator of the American Heart Association. This work was also supported by NIH/NCRR grant (C06 RR018928) to Gladstone Institutes.

Received: March 1, 2007
Revised: March 20, 2007
Accepted: March 22, 2007
Published online: March 29, 2007

REFERENCES

Ambros, V. (2004). The functions of animal microRNAs. Nature *431*, 350–355.

Berezikov, E., Thuemmler, F., van Laake, L.W., Kondova, I., Bontrop, R., Cuppen, E., and Plasterk, R.H. (2006). Diversity of microRNAs in human and chimpanzee brain. Nat. Genet. *38*, 1375–1377.

Bernstein, E., Caudy, A.A., Hammond, S.M., and Hannon, G.J. (2001). Role for a bidentate ribonuclease in the initiation step of RNA interference. Nature *409*, 363–366.

Birmingham, A., Anderson, E.M., Reynolds, A., Ilsley-Tyree, D., Leake, D., Fedorov, Y., Baskerville, S., Maksimova, E., Robinson, K., Karpilow, J., et al. (2006). 3′ UTR seed matches, but not overall identity, are associated with RNAi off-targets. Nat. Methods *3*, 199–204.

Brennecke, J., Hipfner, D.R., Stark, A., Russell, R.B., and Cohen, S.M. (2003). bantam encodes a developmentally regulated microRNA that controls cell proliferation and regulates the proapoptotic gene hid in Drosophila. Cell *113*, 25–36.

Brennecke, J., Stark, A., Russell, R.B., and Cohen, S.M. (2005). Principles of microRNA-target recognition. PLoS Biol. *3*, e85.

Buckingham, M., Meilhac, S., and Zaffran, S. (2005). Building the mammalian heart from two sources of myocardial cells. Nat. Rev. Genet. *6*, 826–835.

Chen, J.F., Mandel, E.M., Thomson, J.M., Wu, Q., Callis, T.E., Hammond, S.M., Conlon, F.L., and Wang, D.Z. (2006). The role of microRNA-1 and microRNA-133 in skeletal muscle proliferation and differentiation. Nat. Genet. *38*, 228–233.

Cheng, C.F., Kuo, H.C., and Chien, K.R. (2003). Genetic modifiers of cardiac arrhythmias. Trends Mol. Med. *9*, 59–66.

Cohen, S.M., Brennecke, J., and Stark, A. (2006). Denoising feedback loops by thresholding–a new role for microRNAs. Genes Dev. *20*, 2769–2772.

Costantini, D.L., Arruda, E.P., Agarwal, P., Kim, K.-H., Zhu, Y., Lebel, M., Cheng, C.W., Park, C.Y., Pierce, S., Guerchicoff, A., et al. (2005). The homeodomain transcription factor Irx5 establishes the mouse cardiac ventricular repolarization gradient. Cell *123*, 347–358.

Desai, A.D., Yaw, T.S., Yamazaki, T., Kaykha, A., Chun, S., and Froelicher, V.F. (2006). Prognostic Significance of Quantitative QRS Duration. Am. J. Med. *119*, 600–606.

Didiano, D., and Hobert, O. (2006). Perfect seed pairing is not a generally reliable predictor for miRNA-target interactions. Nat. Struct. Mol. Biol. *13*, 849–851.

Du, T., and Zamore, P.D. (2005). microPrimer: The biogenesis and function of microRNA. Development *132*, 4645–4652.

Fischer, A., and Gessler, M. (2003). Hey genes in cardiovascular development. Trends Cardiovasc. Med. *13*, 221–226.

Garg, V., Kathiriya, I.S., Barnes, R., Schluterman, M.K., King, I.N., Butler, C.A., Rothrock, C.R., Eapen, R.S., Hirayama-Yamada, K., Joo, K., et al. (2003). GATA4 mutations cause human congenital heart defects and reveal an interaction with TBX5. Nature *424*, 443–447.

Garg, V., Muth, A.N., Ransom, J.F., Schluterman, M.K., Barnes, R., King, I.N., Grossfeld, P.D., and Srivastava, D. (2005). Mutations in NOTCH1 cause aortic valve disease. Nature *437*, 270–274.

Gottlieb, P.D., Pierce, S.A., Sims, R.J., Yamagishi, H., Weihe, E.K., Harriss, J.V., Maika, S.D., Kuziel, W.A., King, H.L., Olson, E.N., et al. (2002). Bop encodes a muscle-restricted protein containing MYND and SET domains and is essential for cardiac differentiation and morphogenesis. Nat. Genet. *31*, 25–32.

Gourdie, R.G., Kubalak, S., and Mikawa, T. (1999). Conducting the embryonic heart: Orchestrating development of specialized cardiac tissues. Trends Cardiovasc. Med. *9*, 18–26.

Harfe, B.D., McManus, M.T., Mansfield, J.H., Hornstein, E., and Tabin, C.J. (2005). The RNaseIII enzyme Dicer is required for morphogenesis but not patterning of the vertebrate limb. Proc. Natl. Acad. Sci. USA *102*, 10898–10903.

Hoffman, J.I., Kaplan, S., and Liberthson, R.R. (2004). Prevalence of congenital heart disease. Am. Heart J. *147*, 425–439.

Hornstein, E., Mansfield, J.H., Yekta, S., Hu, J.K., Harfe, B.D., McManus, M.T., Baskerville, S., Bartel, D.P., and Tabin, C.J. (2005). The microRNA miR-196 acts upstream of Hoxb8 and Shh in limb development. Nature *438*, 671–674.

Jackson, A.L., Burchard, J., Schelter, J., Chau, B.N., Cleary, M., Lim, L., and Linsley, P.S. (2006). Widespread siRNA "off-target" transcript silencing mediated by seed region sequence complementarity. RNA *12*, 1179–1187.

Johnston, R.J., and Hobert, O. (2003). A microRNA controlling left/right neuronal asymmetry in Caenorhabditis elegans. Nature *426*, 845–849.

Kim, H.K., Lee, Y.S., Sivaprasad, U., Malhotra, A., and Dutta, A. (2006). Muscle-specific microRNA miR-206 promotes muscle differentiation. J. Cell Biol. *174*, 677–687.

Kloosterman, W.P., and Plasterk, R.H. (2006). The diverse functions of microRNAs in animal development and disease. Dev. Cell *11*, 441–450.

Koo, B.-K., Lim, H.-S., Song, R., Yoon, M.-J., Yoon, K.-J., Moon, J.-S., Kim, Y.-W., Kwon, M.-C., Yoo, K.-W., Kong, M.-P., et al. (2005). Mind bomb 1 is essential for generating functional Notch ligands to activate Notch. Development *132*, 3459–3470.

Kwon, C., Han, Z., Olson, E.N., and Srivastava, D. (2005). MicroRNA1 influences cardiac differentiation in Drosophila and regulates Notch signaling. Proc. Natl. Acad. Sci. USA *102*, 18986–18991.

Lagos-Quintana, M., Rauhut, R., Lendeckel, W., and Tuschl, T. (2001). Identification of novel genes coding for small expressed RNAs. Science *294*, 853–858.

Lee, R.C., Feinbaum, R.L., and Ambros, V. (1993). The *C. elegans* heterochronic gene lin-4 encodes small RNAs with antisense complementarity to lin-14. Cell *75*, 843–854.

Lewis, B.P., Burge, C.B., and Bartel, D.P. (2005). Conserved seed pairing, often flanked by adenosines, indicates that thousands of human genes are microRNA targets. Cell *120*, 15–20.

Li, F., Wang, X., Capasso, J.M., and Gerdes, A.M. (1996). Rapid transition of cardiac myocytes from hyperplasia to hypertrophy during postnatal development. J. Mol. Cell. Cardiol. *28*, 1737–1746.

Liao, J., Kochilas, L., Nowotschin, S., Arnold, J.S., Aggarwal, V.S., Epstein, J.A., Brown, M.C., Adams, J., and Morrow, B.E. (2004). Full spectrum of malformations in velo-cardio-facial syndrome/DiGeorge syndrome mouse models by altering Tbx1 dosage. Hum. Mol. Genet. *13*, 1577–1585.

Lim, L.P., Lau, N.C., Garrett-Engele, P., Grimson, A., Schelter, J.M., Castle, J., Bartel, D.P., Linsley, P.S., and Johnson, J.M. (2005). Microarray analysis shows that some microRNAs downregulate large numbers of target mRNAs. Nature *433*, 769–773.

MacLellan, W.R., and Schneider, M.D. (2000). Genetic dissection of cardiac growth control pathways. Annu. Rev. Physiol. *62*, 289–319.

McFadden, D.G., Barbosa, A.C., Richardson, J.A., Schneider, M.D., Srivastava, D., and Olson, E.N. (2005). The Hand1 and Hand2 transcription factors regulate expansion of the embryonic cardiac ventricles in a gene dosage-dependent manner. Development *132*, 189–201.

Moses, K.A., DeMayo, F., Braun, R.M., Reecy, J.L., and Schwartz, R.J. (2001). Embryonic expression of an Nkx2-5/Cre gene using ROSA26 reporter mice. Genesis *31*, 176–180.

Moss, E.G., Lee, R.C., and Ambros, V. (1997). The cold shock domain protein LIN-28 controls developmental timing in *C. elegans* and is regulated by the lin-4 RNA. Cell *88*, 637–646.

Nakagawa, O., Nakagawa, M., Richardson, J.A., Olson, E.N., and Srivastava, D. (1999). HRT1, HRT2, and HRT3: A new subclass of bHLH transcription factors marking specific cardiac, somitic, and pharyngeal arch segments. Dev. Biol. *216*, 72–84.

Olson, E.N. (2006). Gene regulatory networks in the evolution and development of the heart. Science *313*, 1922–1927.

Rajewsky, N. (2006). microRNA target predictions in animals. Nat. Genet. Suppl. *38*, S8–S13.

Rao, P.K., Kumar, R.M., Farkhondeh, M., Baskerville, S., and Lodish, H.F. (2006). Myogenic factors that regulate expression of muscle-specific microRNAs. Proc. Natl. Acad. Sci. USA, in press.

Redon, R., Ishikawa, S., Fitch, K.R., Feuk, L., Perry, G.H., Andrews, T.D., Fiegler, H., Shapero, M.H., Carson, A.R., Chen, W., et al. (2006). Global variation in copy number in the human genome. Nature *444*, 444–454.

Reinhart, B.J., Slack, F.J., Basson, M., Pasquinelli, A.E., Bettinger, J.C., Rougvie, A.E., Horvitz, H.R., and Ruvkun, G. (2000). The 21-nucleotide let-7 RNA regulates developmental timing in *Caenorhabditis elegans*. Nature *403*, 901–906.

Sayed, D., Hong, C., Chen, I.Y., Lypowy, J., and Abdellatif, M. (2007). MicroRNAs play an essential role in the development of cardiac hypertrophy. Circ. Res. *100*, 416–424.

Shin, C.H., Liu, Z.P., Passier, R., Zhang, C.L., Wang, D.Z., Harris, T.M., Yamagishi, H., Richardson, J.A., Childs, G., and Olson, E.N. (2002). Modulation of cardiac growth and development by HOP, an unusual homeodomain protein. Cell *110*, 725–735.

Sokol, N.S., and Ambros, V. (2005). Mesodermally expressed *Drosophila* microRNA-1 is regulated by Twist and is required in muscles during larval growth. Genes Dev. *19*, 2343–2354.

Soonpaa, M.H., and Field, L.J. (1998). Survey of studies examining mammalian cardiomyocyte DNA synthesis. Circ. Res. *83*, 15–26.

Srivastava, D. (2006). Making or breaking the heart: From lineage determination to morphogenesis. Cell *126*, 1037–1048.

Srivastava, D., Cserjesi, P., and Olson, E.N. (1995). A subclass of bHLH proteins required for cardiac morphogenesis. Science *270*, 1995–1999.

Srivastava, D., Thomas, T., Lin, Q., Kirby, M.L., Brown, D., and Olson, E.N. (1997). Regulation of cardiac mesodermal and neural crest development by the bHLH transcription factor, dHAND. Nat. Genet. *16*, 154–160.

Stark, A., Brennecke, J., Russell, R.B., and Cohen, S.M. (2003). Identification of *Drosophila* MicroRNA targets. PLoS Biol. *1*, E60.

Thom, T., Haase, N., Rosamond, W., Howard, V.J., Rumsfeld, J., Manolio, T., Zheng, Z.J., Flegal, K., O'Donnell, C., Kittner, S., et al. (2006). Heart disease and stroke statistics–2006 update: A report from the American Heart Association Statistics Committee and Stroke Statistics Subcommittee. Circulation *113*, e85–e151.

Torella, D., Ellison, G.M., Mendez-Ferrer, S., Ibanez, B., and Nadal-Ginard, B. (2006). Resident human cardiac stem cells: role in cardiac cellular homeostasis and potential for myocardial regeneration. Nat. Clin. Pract. Cardiovasc. Med. *3*, S83–S89.

Valencia-Sanchez, M.A., Liu, J., Hannon, G.J., and Parker, R. (2006). Control of translation and mRNA degradation by miRNAs and siRNAs. Genes Dev. *20*, 515–524.

van Rooij, E., Sutherland, L.B., Liu, N., Williams, A.H., McAnally, J., Gerard, R.D., Richardson, J.A., and Olson, E.N. (2006). A signature pattern of stress-responsive microRNAs that can evoke cardiac hypertrophy and heart failure. Proc. Natl. Acad. Sci. USA *103*, 18255–18260.

Vella, M.C., Choi, E.Y., Lin, S.Y., Reinert, K., and Slack, F.J. (2004). The C. elegans microRNA let-7 binds to imperfect let-7 complementary sites from the lin-41 3′UTR. Genes Dev. *18*, 132–137.

Wei, Y., Mizzen, C.A., Cook, R.G., Gorovsky, M.A., and Allis, C.D. (1998). Phosphorylation of histone H3 at serine 10 is correlated with chromosome condensation during mitosis and meiosis in Tetrahymena. Proc. Natl. Acad. Sci. USA *95*, 7480–7484.

Wienholds, E., Kloosterman, W.P., Miska, E., Alvarez-Saavedra, E., Berezikov, E., de Bruijn, E., Horvitz, H.R., Kauppinen, S., and Plasterk, R.H. (2005). MicroRNA expression in zebrafish embryonic development. Science *309*, 310–311.

Wightman, B., Ha, I., and Ruvkun, G. (1993). Posttranscriptional regulation of the heterochronic gene lin-14 by lin-4 mediates temporal pattern formation in *C. elegans*. Cell *75*, 855–862.

Xie, X., Lu, J., Kulbokas, E.J., Golub, T.R., Mootha, V., Lindblad-Toh, K., Lander, E.S., and Kellis, M. (2005). Systematic discovery of regulatory motifs in human promoters and 3′ UTRs by comparison of several mammals. Nature *434*, 338–345.

Xin, M., Davis, C.A., Molkentin, J.D., Lien, C.L., Duncan, S.A., Richardson, J.A., and Olson, E.N. (2006). A threshold of GATA4 and GATA6 expression is required for cardiovascular development. Proc. Natl. Acad. Sci. USA *103*, 11189–11194.

Yamagishi, H., Yamagishi, C., Nakagawa, O., Harvey, R.P., Olson, E.N., and Srivastava, D. (2001). The combinatorial activities of Nkx2.5 and dHAND are essential for cardiac ventricle formation. Dev. Biol. *239*, 190–203.

Yamagishi, H., Maeda, J., Hu, T., McAnally, J., Conway, S.J., Kume, T., Meyers, E.N., Yamagishi, C., and Srivastava, D. (2003). Tbx1 is regulated by tissue-specific forkhead proteins through a common Sonic hedgehog-responsive enhancer. Genes Dev. *17*, 269–281.

Yelon, D., Ticho, B., Halpern, M.E., Ruvinsky, I., Ho, R.K., Silver, L.M., and Stainier, D.Y. (2000). The bHLH transcription factor hand2 plays parallel roles in zebrafish heart and pectoral fin development. Development *127*, 2573–2582.

Yi, R., O'Carroll, D., Pasolli, H.A., Zhang, Z., Dietrich, F.S., Tarakhovsky, A., and Fuchs, E. (2006). Morphogenesis in skin is governed by discrete sets of differentially expressed microRNAs. Nat. Genet. *38*, 356–362.

Zhao, Y., Samal, E., and Srivastava, D. (2005). Serum response factor regulates a muscle-specific mircroRNA that targets *Hand2* during cardiogenesis. Nature *436*, 214–220.

Zhao, Y., and Srivastava, D. (2007). A developmental view of microRNA function. Trends Biochem. Sci., in press. Published online March 8, 2007. 10.1016/j.tibs.2007.1002.1006.

Zipes, D.P., and Wellens, H.J. (1998). Sudden cardiac death. Circulation *98*, 2334–2351.

Accession Numbers

Microarray data have been submitted and can be accessed by GEO accession numbers GSE7333 and GSE7343.